Simultaneous Electrochemical Reduction and Delamination of Graphene Oxide Films

Xiaohan Wang,[†] Iskandar Kholmanov,[*,†,‡] Harry Chou,[†] and Rodney S. Ruoff[*,†,§]

[†]Materials Science and Engineering Program, University of Texas at Austin, Austin, Texas 78712, United States, [‡]CNR-INO Brescia, Sensor Lab, Via Branze 45, 25123 Brescia, Italy, and [§]Center for Multidimensional Carbon Materials, Institute of Basic Sciences Center, Ulsan National Institute of Science and Technology, Ulsan, 689-798, Republic of Korea

ABSTRACT Here we report an electrochemical method to simultaneously reduce and delaminate graphene oxide (G-O) thin films deposited on metal (Al and Au) substrates. During the electrochemical reaction, interface charge transfer between the G-O thin film and the electrode surface was found to be important in eliminating oxygen-containing groups, yielding highly reduced graphene oxide (rG-O). In the meantime, hydrogen bubbles were electrochemically generated at the rG-O film/electrode interface, propagating the film delamination. Unlike other metal-based G-O reduction methods, the metal used here was either not etched at all (for Au) or etched a small amount (for Al), thus making it possible to reuse the substrate and lower production costs. The delaminated rG-O film exhibits a thickness-dependent degree of reduction: greater reduction is achieved in thinner films. The thin rG-O films having an optical transmittance of 90% ($\lambda = 550$ nm) had a sheet resistance of 6390 $\pm$ 447 Ω/□ (ohms per square). rG-O-based stretchable transparent conducting films were also demonstrated.

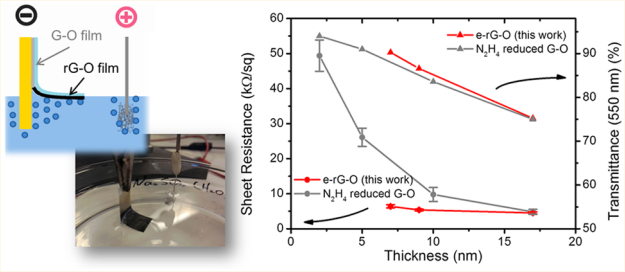

KEYWORDS: graphene oxide · electrochemical reduction · transparent conducting films · stretchable electronics

Graphene oxide (G-O), obtained by exfoliation of graphite oxide, is defined here as an individual layer of graphite oxide. Reduction of G-O (which gives "rG-O") removes the majority of oxygen-containing functional groups and increases its electrical conductivity. Due to its high flexibility and unique optical properties, rG-O thin films are attractive for emerging thin-film electronic and optoelectronic device applications.[1−4] Currently, rG-O thin films are mainly fabricated through two routes: (i) reduction of predeposited G-O films or (ii) deposition of reduced G-O dispersions.[5]

For the first route, three major reduction methods are available: thermal treatment, chemical reduction, and electrochemical reduction. To achieve highly reduced G-O films by thermal treatment, high temperatures (>1000 °C) and ultrahigh vacuum (or a reducing environment) are required.[6−8] Such conditions are not compatible with most polymer substrates. In the case of chemical reduction, reducing agents such as hydrazine,[8−10] *N*,*N*-dimethylhydrazine,[11] and sodium borohydride[12] have been used for deoxygenation, and because of their toxic properties, safety precautions must be taken when large quantities of these reagents are used. Electrochemical reduction involves changing the Fermi energy level of the electrode material surface and thus direct charge transfer is used to efficiently reduce G-O films on the electrode surface.[13,14] However, due to the high hydrophilicity of G-O sheets, unsupported G-O films can easily dissociate in aqueous solutions. Water intercalation usually happens,[15] and this adversely affects the initial structure, especially for ultrathin films.

As for the route of depositing rG-O dispersion, the aforementioned harsh reducing agents are undesirable in terms of safety. Recently, mild reducing metal particles (Fe, Zn, and Al)[16−18] were reported as "green" chemical reduction agents for G-O, but the amount of the rG-O obtained is limited by the amount of metal particles that are consumed during this process.[17]

* Address correspondence to ruofflab@gmail.com (R.S.R.), iskandar.kholmanov@austin.utexas.edu (I.K.).

Received for review January 27, 2015 and accepted August 8, 2015.

Published online August 08, 2015
10.1021/acsnano.5b03814

Moreover, such reduction processes alter the hydrophilicity of G-O sheets dispersed in aqueous solutions,[19] and the resulting agglomeration of rG-O sheets is detrimental for both film fabrication and performance.[20]

Here we report a new method that simultaneously reduces and delaminates predeposited G-O films on metal substrates. This method involves features of electrochemical reduction[13,14] and a CVD (chemical vapor deposition)-graphene transfer method known as 'electrochemical delamination'.[21,22] Electrons transport from a metal surface to both G-O sheets and hydrogen ions in solution, forming rG-O and hydrogen bubbles, respectively. The bubbles promote delamination of the film without affecting its integrity. It was found that the reduction of a G-O film depends on its thickness; the C/O atomic ratio changes with respect to the distance from the electrode surface. Ultrathin rG-O films with high optical transmittance and good electrical conductivity were obtained, suitable for transparent conducting film (TCF) applications. This method can, in principle, be scaled-up to produce very large-area rG-O films on arbitrary substrates, including those that are stretchable and flexible. Unlike other metal-based reduction methods, the metal substrate in this approach is preserved for reuse.

RESULTS AND DISCUSSION

A dispersion of G-O platelets was prepared by dispersing graphite oxide made by a modified Hummers' method;[11] this dispersion was then spin-coated on a metal substrate, which acts as an electrode in the following electrochemical setup. Two different metal substrates were used in order to better understand the mechanism of G-O reduction and control for any effect due to the electrode material: one was Al foil, an active metal, as shown in Figure 1 (with and without electropolishing treatment), and the second was Au film (on silicon wafer), a noble metal, shown in Supporting Information (SI) Movie M1. By varying the G-O concentration and the spin-coating speed, the film thickness was adjusted from a few to hundreds of nanometers. A removable poly(methyl methacrylate) (PMMA) capping layer was spin-coated atop of the G-O film to maintain the film integrity (SI Figure S1).

For the reduction/delamination process (Figure 1a), an electrolytic cell was made with PMMA/G-O/metal substrate as the cathode and a Pt mesh as the anode. Aqueous Na_2SO_4 solution (0.5 M) was used as the electrolyte. A 10−15 V direct current voltage was then applied across the cell electrodes; this caused the light-yellow G-O film to immediately blacken at the film edges. This change in color indicates reduction of the G-O film by elimination of oxygen-containing groups and restoration of sp^2 carbon bonds.[13] Simultaneously, hydrogen bubbles were produced at the edges by the electrolysis of water: $2H_2O\,(l) + 2e^- \rightarrow H_2\,(g) + 2OH^-\,(aq)$.

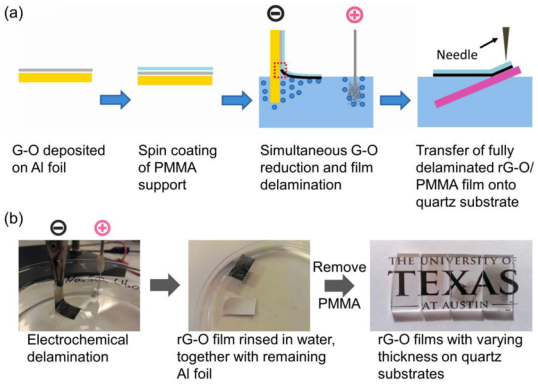

Figure 1. Simultaneous reduction/delamination of predeposited G-O film on a polished Al substrate. (a) Schematic illustration of PMMA-supported film fabrication. Reduction of G-O film occurs at the triple-phase (metal/G-O/electrolyte solution) interline (dashed red rectangle). (b) Optical images corresponding to key experimental steps. The entire reduction/delamination process is completed in 10 min for a 1 × 2.5 cm^2 film.

The bubbles gently and continuously delaminated the reduced G-O film (with supporting PMMA layer) from the electrode surface. This simultaneous reduction and delamination process was completed in a few minutes (Figure 1b), as opposed to other hours-long metal-based reduction processes.[16] More importantly, unlike other metal-based reduction methods where the metal is dissolved completely,[16−18] the metal foil used here is not etched (for Au) or only partially etched (for Al, ~0.25 mg/cm^2 per cycle). This enables us to reuse the electrode material (see SI for detailed discussion), making the approach suitable for low-cost rG-O film fabrication. The delaminated PMMA/rG-O film was then rinsed with distilled water and transferred onto the target substrate. The capping PMMA layer was removed by soaking in acetone for 8 h. If the desired final target substrate is a castable polymer, the film fabrication process can be further simplified by directly casting that target substrate on the deposited G-O film, as shown below for a polydimethylsiloxane (PDMS) substrate.

To understand the mechanism responsible for our G-O reduction method, we first consider two previously reported metal-based reduction mechanisms: (i) reduction due to the direct charge transfer between metal and G-O sheets[13,14] and (ii) reduction by nascent hydrogen atoms (which are hydrogen atoms at the moment of formation) produced on the metal surface.[23] With respect to our experiments, we found that G-O reduction did not occur when unpolished Al foils were used as metal substrates, even though hydrogen bubbles were still present. Considering that Al foil inevitably forms a native surface oxide layer that is inefficient for electron transport (insulating), we speculate that direct charge transfer is responsible for G-O reduction in our simultaneous reduction/delamination process. When electropolished Al foil (with thinner oxide layer) or Au-coated wafer (with no oxide layer)

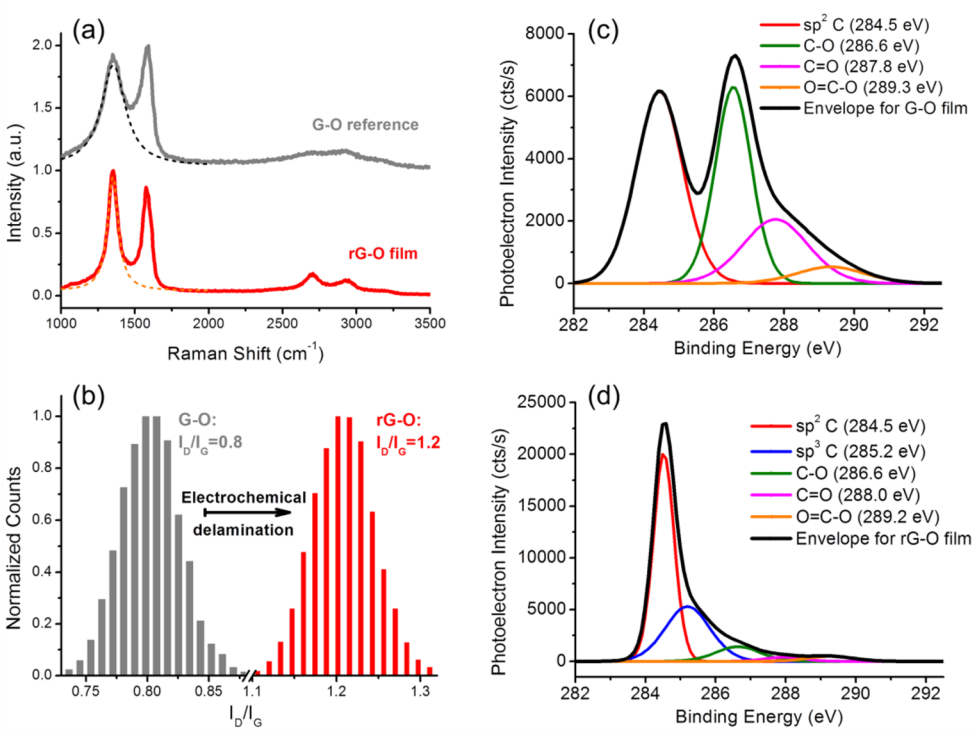

Figure 2. Characterization of G-O reduction. (a) Raman spectra of the G-O reference and the reduced G-O film on quartz substrate. D bands are fitted to Lorentzian curves (dashed). (b) Histogram distributions extracted from Raman map data for I_D/I_G (SI Figure S3) before and after reduction. (c and d) XPS C 1s spectrum of G-O film before and after electrochemical reduction/delamination. A Gaussian/Lorentzian fit is shown.

was used, electrons could efficiently transport across the G-O/metal substrate interface and promote the following electrode reaction: G-O + aH_2O + $be^- \rightarrow$ rG-O + bOH^-.[13] A triple-phase (electrode/G-O/electrolyte solution) interline which is highlighted by a dashed red rectangle in Figure 1a is thus required. With the accompanying evolution of hydrogen bubbles, the interline progressively moves along the G-O/metal interface, providing access to "fresh" (not-reduced) G-O sheets for the solution and subsequent reduction. Compared with the static contact (between G-O film and electrode) method used before,[13] the moving reduction front here is more efficient, particularly when large-area rG-O films are the goal.

Raman spectroscopy (WITec Micro-Raman Spectrometer Alpha 300) was used to characterize the G-O film before and after the reduction process. The characterization results for the rG-O films from both the Al foil and Au film substrates were similar, as shown in Figure 2 and SI Figure S2. Due to the decrease in size of the in-plane sp^2 domains after extensive oxidation and ultrasonic exfoliation,[16] the G-O film exhibits a broad and intense D (~1350 cm^{-1}) band in its Raman spectrum (Figure 2a). However, that prominent D peak significantly narrows in the delaminated rG-O film, with the full width at half maximum (FWHM) decrease from 188 to 80 cm^{-1}. This compares favorably with values for other chemically or thermally reduced G-O films and corresponds to a low fraction of carbon atoms (<20%) that are not sp^2 hybridized.[24] By extracting and analyzing Raman data from a 30 × 30 μm^2 map (SI Figure S3), the relative intensity of the D (*K*-point phonons of A_{1g} symmetry) and G (~1580 cm^{-1}, zone center phonons of E_{2g} symmetry) bands (I_D/I_G) was found to increase from 0.8 to 1.2 (Figure 2b). The histogram shows that the rG-O film is homogeneous over the scanned area, while the I_D/I_G increase is consistent with other G-O reduction methods.[16,25]

The change in chemical composition of the G-O films during the reduction/delamination process was characterized by X-ray photoelectron spectroscopy (XPS; see Materials and Methods). Figure 2c shows the C 1s spectrum of a spin-coated G-O film on a quartz substrate. By applying a Gaussian−Lorentzian peak fitting, four peaks centered at 284.5, 286.6, 287.8, and 289.3 eV are observed. These peaks correspond to sp^2 carbon, epoxide/ether, carbonyl, and carboxyl groups, respectively,[16] and show the large amounts of heavily oxidized G-O platelets. In contrast, the peaks associated with the oxygen functionalities are significantly suppressed in the rG-O film obtained by our electrochemical approach (Figure 2d). This is consistent with a high degree of removal of oxygen-containing groups. Also, beside the peak of sp^2 carbon, a small peak (285.2 eV) assigned to sp^3 carbon appears. This is likely due to a uniformly reduced G-O film after delamination, leading to a narrower sp^2 peak and less peak overlap.[26] According to the survey spectra

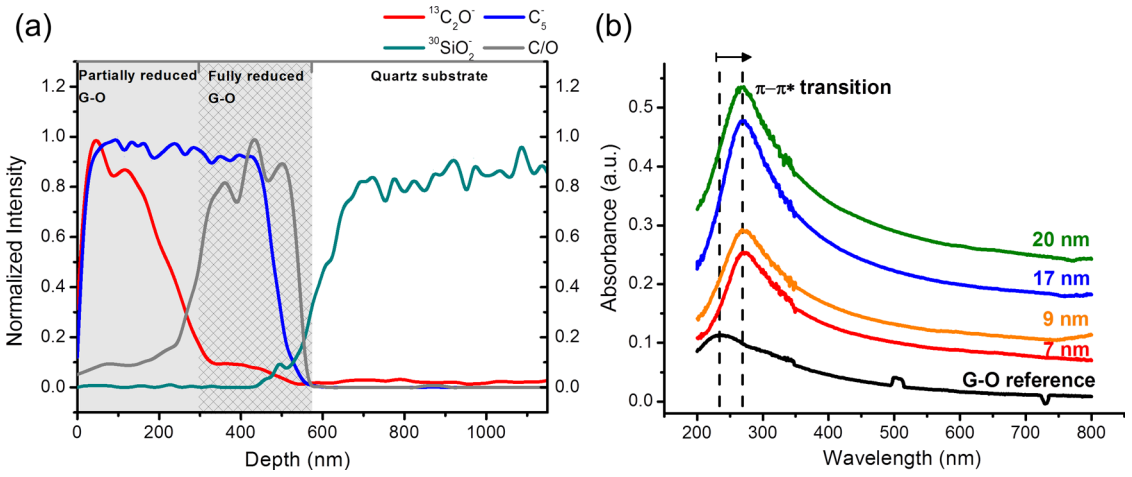

Figure 3. (a) TOF-SIMS depth profiles of normalized secondary ion species within a 550 nm thick rG-O film on a quartz substrate. The ratio of carbon and oxygen (C/O) is used to indicate various degrees of reduction. Based on this, the film is divided by partially reduced (shaded gray) and fully reduced (shaded cross-hatched pattern) regions. (b) UV−vis spectra of G-O reference and rG-O films with different thicknesses. The red shift of peak position corresponds to recovery of conjugated structures.

(SI Figure S4), the atomic ratio of carbon and oxygen (C/O) was found to increase from 2.89 (for G-O) to 9.26 (for rG-O) after electrochemical reduction/delamination. This value is among the best reported for G-O reduced by other methods.[16]

Due to the aforementioned charge transfer between the electrode and G-O during the reduction/delamination process, the reduction is found to be thickness-dependent: a higher degree of reduction was noted at the electrode/G-O interface. This was confirmed by TOF-SIMS (Time-of-Flight Secondary Ion Mass Spectrometry) depth profiling through a 550 nm thick rG-O film (Figure 3a). For this experiment, delaminated PMMA/rG-O was transferred onto a quartz substrate with the highly reduced G-O surface facing down. PMMA was subsequently removed in acetone. The depth profiling (conditions described in Materials and Methods) penetrated about 1100 nm into the sample and substrate (550 nm rG-O and 550 nm quartz, as shown in Figure 3a). The normalized TOF-SIMS depth profile of the C_5^- species (blue curve representing carbon) is roughly constant in rG-O, and then it abruptly decreases at the rG-O/quartz interface. In contrast, the $^{13}C_2O^-$ species (red curve representing oxygen) remains constant only for the topmost 120 nm of the film and gradually decreases with increasing depth of penetration. It reaches a floor at around 300 nm and remains constant until the interface (indicated by the increase in silicon species, green curve). A calculated C/O profile (gray curve using the C_5^- and $^{13}C_2O^-$ species) obtained from the carbon and oxygen signals shows the variation in the reduction of the film through its thickness. The profile demonstrates that the G-O film is highly and homogeneously reduced for a film thickness of up to 200 nm. For films with a thickness higher than 200 nm, the degree of reduction (C/O) gradually decreases.

The thickness-dependent C/O ratio variation is attributed to the parallel G-O reduction and hydrogen evolution on the cathode surface. At the triple-phase interline, G-O sheets in direct contact with the electrode are first reduced by electrochemical reaction due to its less negative redox potential compared with hydrogen evolution. As the reduction proceeds through the film thickness, the overpotential for G-O reduction becomes higher due to the less efficient electron transport in the rG-O part than that in the metal electrode. As a consequence, the hydrogen evolution becomes more significant and causes the film to be delaminated by hydrogen bubbles. The delamination cuts off the electron pathway from the metal to the rG-O and terminates further G-O reduction; thus, the full thickness of the film is not completely reduced. These results show that the reduction/delamination approach works especially well for fabricating thin (<200 nm thick for our case) rG-O films.

This observation is also consistent with UV−vis spectroscopy studies of the films of different thicknesses. As the film thickness is varied from a few to tens of nanometers, the absorption peaks in UV−vis spectra associated with $\pi-\pi^*$ transition show a consistent shift from 235 nm (for G-O) to 270 nm (for rG-O), for all measured films, as shown in Figure 3b. This suggests an efficient and homogeneous reduction of these thin G-O films,[16] independent of their thickness (as they are all thinner than our 200 nm threshold thickness).

Simultaneous reduction and delamination of G-O is particularly suitable for fabricating TCFs. Figure 4a shows the TCF characteristics of G-O films reduced by electrochemical reduction/delamination (e-rG-O), compared with hydrazine (100 °C for 24 h) reduced G-O films (h-rG-O, extracted from ref 10). In comparison

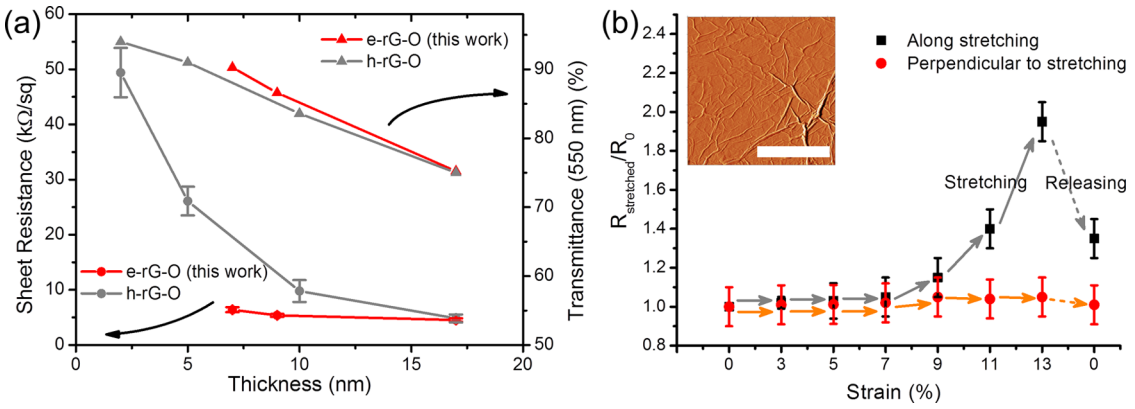

Figure 4. (a) Sheet resistance and optical transmittance of G-O films reduced by hydrazine (gray) or electrochemical delamination (red). (b) Changes in sheet resistance during stretching of the substrate. The arrows mark the order of the measurements. The high density of wrinkles in as-prepared rG-O films is shown in the inset AFM image (with a scale bar of 2 μm), which contributes to the good electrical properties up to a strain of 7%.

with h-rG-O films of the same thickness and transmittance, the e-rG-O film possesses lower sheet resistance. This can be ascribed to a higher degree of G-O reduction.[12] A sheet resistance of 6.4 kΩ/□ (ohms per square) and an optical transmittance of 90% (λ = 550 nm) were achieved. This combination is superior to most rG-O TCFs[5] and suitable for touch screen and photovoltaic devices.[2,27]

This PMMA-supported G-O reduction/delamination process is compatible with rG-O film fabrication on flexible substrates. Alternatively, the intermediate PMMA support can be eliminated if the desired final target substrate is a castable polymer. As a demonstration, G-O film on Al foil was first spin coated with a layer of PDMS (50 μm thick). The G-O film was then simultaneously reduced and delaminated by the same electrochemical process (SI Figure S5), yielding rG-O film on a PDMS substrate. This structure allows for electromechanical testing of the rG-O film by stretching the PDMS substrate (Figure 4b). Stretching the structure up to 7% strain showed no significant sheet resistance changes along the stretching direction, which is much better than what was observed in the CVD graphene case.[28] Atomic force microscopy (AFM, inset of Figure 4b) and scanning electron microscopy (SEM, SI Figure S1) show a random distribution of wrinkles within the as-prepared rG-O films. Reportedly, these structures contribute to an enhancement of film electromechanical properties.[28] Moreover, the sliding of overlapped and stacked rG-O platelets in the film is also well demonstrated,[29] and this is beneficial for mechanical stability.[30] Further stretching resulted in a gradual increase in resistance. The film resistance almost doubled with a strain of 13%. The electrical properties of the samples stretched up to a strain of 11% were recovered after releasing and remained consistent even after tens of stretching cycles.

CONCLUSIONS

In summary, a highly effective electrochemical approach is reported for simultaneous reduction and delamination of G-O films. The electron transport across the G-O/electrode interface was found to be important for G-O reduction, and the extent of reduction depends on the film thickness. Hydrogen bubbles are produced at the rG-O/electrode interface, which delaminate the film from the metal substrate. Using this method, homogeneously reduced G-O films with thicknesses up to 200 nm were prepared on arbitrary substrates. This approach is compatible with scaling-up to produce large-area thin rG-O films with good electrical conductivity and high optical transmittance. This is suitable for TCF applications. Compared to other chemical or electrochemical reduction methods, our approach is green and particularly straightforward and may impact future rG-O film techniques.

MATERIALS AND METHODS

Electropolishing of Al Foil. Al foil (purchased from Boardwalk, 20-μm thick) was employed as an anode in an electrolytic cell with an Al plate as the cathode. The electrolyte solution was prepared by mixing 100 mL of water, 50 mL of ethanol, 10 mL of isopropyl alcohol, 50 mL of phosphoric acid, and 1 g of urea. A Hewlett-Packard 612 System DC power supply applied a constant potential of 6 V for 1 min, followed by Al foil washing with distilled water and ethanol. A glass substrate (1 × 1 in.^{2}), as a rigid support, was then attached to the polished Al foil.

Au Electrode. A 50 nm-thick Au film was e-beam evaporated onto an acetone/IPA treated Si wafer at a rate of 0.5 Å/s under a pressure of 5×10^{-6} mbar.

XPS Measurement. A Kratos Axis Ultra XPS was used to determine the chemical composition of G-O films. The X-ray source used was a monochromated Al K_α ($h\nu$ = 1486.5 eV), and the optics were a hybrid with both immersion magnetic and electrostatic lenses. The photoelectrons were collected with a multichannel plate and delay line detector coupled to a hemispherical analyzer.

TOF-SIMS Depth Profiling. A TOF.SIMS 5 from ION-TOF GmbH was used here. The depth profile was obtained using two interlaced ion sources; a 1 kV Cs^+ "sputter" beam and a 30 kV Bi^+ "analysis" beam. Negative secondary ions were collected in the time-of-flight mass analyzer. Species C_5^- and $^{13}C_2O^-$ are used to track carbon and oxygen in the rG-O film, respectively, whereas $^{30}SiO_2^-$ represents the quartz substrate. These species are selected due to their signal intensity (to avoid saturating the detector while still generating sufficient counts), mass resolution (free from mass interference with other ions), and correlating well with the structure of the sample itself (for example, O^- and $^{18}O^-$ appear in the substrate as well as rG-O but $^{13}C_2O^-$ appears only in the rG-O).

Sheet Resistance Measurement. Sheet resistance values were obtained using the standard four-probe van der Pauw method. Four gold electrodes were deposited in a configuration that leaves a square film with a size approximately 0.5 × 0.5 cm^2. For electrical resistance measurements under stretching, a 1.5 × 0.5 cm^2 rG-O film with a PDMS supporting layer was transferred onto another 1-mm-thick PDMS support to form a PDMS/rG-O/PDMS sandwich stack. Between the sandwich layers, four contacts (silver wires) were fixed at the edges of the rG-O films using a silver paste (two contacts to measure the resistance along the stretching direction, and two others in the perpendicular direction). The electromechanical experiments were carried out using a two-probe electrical contact instrument and a precision mechanical system. The resistance values along the stretching direction and perpendicular to it were measured by two separate pieces of equipment.

Conflict of Interest: The authors declare no competing financial interest.

Acknowledgment. We thank Prof. C. Grant Willson and Dr. Longjun Li for valuable discussions and manuscript revision. We thank Feng Lu for providing the Au electrode. We appreciate funding support from the National Science Foundation, under Project No. 1206986; NSF-NASCENT Engineering Research Center (Cooperative Agreement No. EEC-1160494); and the South West Academy of Nanoelectronics (SWAN 2.0, Grant 2013-NE-2400), a Semiconductor Research Corporation program.

Supporting Information Available: The Supporting Information is available free of charge on the ACS Publications website at DOI: 10.1021/acsnano.5b03814.

SEM images; XPS survey spectra and Raman maps; Al recyclability test and its dissolution mechanism; reduction and delamination of predeposited G-O films on Au substrates and their characterization (PDF)

Video of G-O reduction/delamination using Au film on silicon wafer (MPG)

REFERENCES AND NOTES

1. Kholmanov, I. N.; Domingues, S. H.; Chou, H.; Wang, X. H.; Tan, C.; Kim, J. Y.; Li, H. F.; Piner, R.; Zarbin, A. J. G.; Ruoff, R. S. Reduced Graphene Oxide/Copper Nanowire Hybrid Films as High-Performance Transparent Electrodes. *ACS Nano* **2013**, *7*, 1811–1816.
2. Yin, Z. Y.; Sun, S. Y.; Salim, T.; Wu, S. X.; Huang, X.; He, Q. Y.; Lam, Y. M.; Zhang, H. Organic Photovoltaic Devices Using Highly Flexible Reduced Graphene Oxide Films as Transparent Electrodes. *ACS Nano* **2010**, *4*, 5263–5268.
3. Robinson, J. T.; Perkins, F. K.; Snow, E. S.; Wei, Z.; Sheehan, P. E. Reduced Graphene Oxide Molecular Sensors. *Nano Lett.* **2008**, *8*, 3137–3140.
4. Lu, G.; Park, S.; Yu, K.; Ruoff, R. S.; Ocola, L. E.; Rosenmann, D.; Chen, J. Toward Practical Gas Sensing with Highly Reduced Graphene Oxide: A New Signal Processing Method To Circumvent Run-to-Run and Device-to-Device Variations. *ACS Nano* **2011**, *5*, 1154–1164.
5. Eda, G.; Chhowalla, M. Chemically Derived Graphene Oxide: Towards Large-Area Thin-Film Electronics and Optoelectronics. *Adv. Mater.* **2010**, *22*, 2392–2415.
6. Mattevi, C.; Eda, G.; Agnoli, S.; Miller, S.; Mkhoyan, K. A.; Celik, O.; Mastrogiovanni, D.; Granozzi, G.; Garfunkel, E.; Chhowalla, M. Evolution of Electrical, Chemical, and Structural Properties of Transparent and Conducting Chemically Derived Graphene Thin Films. *Adv. Funct. Mater.* **2009**, *19*, 2577–2583.
7. Wang, X.; Zhi, L.; Müllen, K. Transparent, Conductive Graphene Electrodes for Dye-Sensitized Solar Cells. *Nano Lett.* **2008**, *8*, 323–327.
8. Becerril, H. A.; Mao, J.; Liu, Z.; Stoltenberg, R. M.; Bao, Z.; Chen, Y. Evaluation of Solution-Processed Reduced Graphene Oxide Films as Transparent Conductors. *ACS Nano* **2008**, *2*, 463–470.
9. Gilje, S.; Han, S.; Wang, M.; Wang, K.; Kaner, R. B. A Chemical Route to Graphene for Device Applications. *Nano Lett.* **2007**, *7*, 3394–3398.
10. Kholmanov, I. N.; Stoller, M. D.; Edgeworth, J.; Lee, W. H.; Li, H.; Lee, J.; Barnhart, C.; Potts, J. R.; Piner, R.; Akinwande, D.; *et al.* Nanostructured Hybrid Transparent Conductive Films with Antibacterial Properties. *ACS Nano* **2012**, *6*, 5157–5163.
11. Stankovich, S.; Dikin, D. A.; Dommett, G. H. B.; Kohlhaas, K. M.; Zimney, E. J.; Stach, E. A.; Piner, R. D.; Nguyen, S. T.; Ruoff, R. S. Graphene-Based Composite Materials. *Nature* **2006**, *442*, 282–286.
12. Shin, H. J.; Kim, K. K.; Benayad, A.; Yoon, S. M.; Park, H. K.; Jung, I. S.; Jin, M. H.; Jeong, H. K.; Kim, J. M.; Choi, J. Y.; *et al.* Efficient Reduction of Graphite Oxide by Sodium Borohydride and Its Effect on Electrical Conductance. *Adv. Funct. Mater.* **2009**, *19*, 1987–1992.
13. Zhou, M.; Wang, Y. L.; Zhai, Y. M.; Zhai, J. F.; Ren, W.; Wang, F. A.; Dong, S. J. Controlled Synthesis of Large-Area and Patterned Electrochemically Reduced Graphene Oxide Films. *Chem. - Eur. J.* **2009**, *15*, 6116–6120.
14. Shao, Y. Y.; Wang, J.; Engelhard, M.; Wang, C. M.; Lin, Y. H. Facile and Controllable Electrochemical Reduction of Graphene Oxide and Its Applications. *J. Mater. Chem.* **2010**, *20*, 743–748.
15. Dreyer, D. R.; Park, S.; Bielawski, C. W.; Ruoff, R. S. The Chemistry of Graphene Oxide. *Chem. Soc. Rev.* **2010**, *39*, 228–240.
16. Fan, Z. J.; Kai, W.; Yan, J.; Wei, T.; Zhi, L. J.; Feng, J.; Ren, Y. M.; Song, L. P.; Wei, F. Facile Synthesis of Graphene Nanosheets *via* Fe Reduction of Exfoliated Graphite Oxide. *ACS Nano* **2011**, *5*, 191–198.
17. Mei, X. G.; Ouyang, J. Y. Ultrasonication-Assisted Ultrafast Reduction of Graphene Oxide by Zinc Powder at Room Temperature. *Carbon* **2011**, *49*, 5389–5397.
18. Fan, Z. J.; Wang, K.; Wei, T.; Yan, J.; Song, L. P.; Shao, B. An Environmentally Friendly and Efficient Route for the Reduction of Graphene Oxide by Aluminum Powder. *Carbon* **2010**, *48*, 1686–1689.
19. Stankovich, S.; Dikin, D. A.; Piner, R. D.; Kohlhaas, K. A.; Kleinhammes, A.; Jia, Y.; Wu, Y.; Nguyen, S. T.; Ruoff, R. S. Synthesis of Graphene-Based Nanosheets *via* Chemical Reduction of Exfoliated Graphite Oxide. *Carbon* **2007**, *45*, 1558–1565.
20. Zhang, J. L.; Yang, H. J.; Shen, G. X.; Cheng, P.; Zhang, J. Y.; Guo, S. W. Reduction of Graphene Oxide *via* L-Ascorbic Acid. *Chem. Commun.* **2010**, *46*, 1112–1114.
21. Wang, Y.; Zheng, Y.; Xu, X. F.; Dubuisson, E.; Bao, Q. L.; Lu, J.; Loh, K. P. Electrochemical Delamination of CVD-Grown Graphene Film: Toward the Recyclable Use of Copper Catalyst. *ACS Nano* **2011**, *5*, 9927–9933.
22. Wang, X. H.; Tao, L.; Hao, Y. F.; Liu, Z. H.; Chou, H.; Kholmanov, I.; Chen, S. S.; Tan, C.; Jayant, N.; Yu, Q. K.; *et al.* Direct Delamination of Graphene for High-Performance Plastic Electronics. *Small* **2014**, *10*, 694–698.
23. Pham, V. H.; Pham, H. D.; Dang, T. T.; Hur, S. H.; Kim, E. J.; Kong, B. S.; Kim, S.; Chung, J. S. Chemical Reduction of an Aqueous Suspension of Graphene Oxide by Nascent Hydrogen. *J. Mater. Chem.* **2012**, *22*, 10530–10536.
24. Diez-Betriu, X.; Alvarez-Garcia, S.; Botas, C.; Alvarez, P.; Sanchez-Marcos, J.; Prieto, C.; Menendez, R.; de Andres, A. Raman Spectroscopy for the Study of Reduction Mechanisms and Optimization of Conductivity in Graphene Oxide Thin Films. *J. Mater. Chem. C* **2013**, *1*, 6905–6912.

25. Moon, I. K.; Lee, J.; Ruoff, R. S.; Lee, H. Reduced Graphene Oxide by Chemical Graphitization. *Nat. Commun.* **2010**, *1*, 73.
26. Hontoria-Lucas, C.; López-Peinado, A. J.; López-González, J. D.; Rojas-Cervantes, M. L.; Martín-Aranda, R. M. Study of Oxygen-Containing Groups in a Series of Graphite Oxides: Physical and Chemical Characterization. *Carbon* **1995**, *33*, 1585–1592.
27. Wang, J.; Liang, M. H.; Fang, Y.; Qiu, T. F.; Zhang, J.; Zhi, L. J. Rod-Coating: Towards Large-Area Fabrication of Uniform Reduced Graphene Oxide Films for Flexible Touch Screens. *Adv. Mater.* **2012**, *24*, 2874–2878.
28. Kim, K. S.; Zhao, Y.; Jang, H.; Lee, S. Y.; Kim, J. M.; Kim, K. S.; Ahn, J. H.; Kim, P.; Choi, J. Y.; Hong, B. H. Large-Scale Pattern Growth of Graphene Films for Stretchable Transparent Electrodes. *Nature* **2009**, *457*, 706–710.
29. Dikin, D. A.; Stankovich, S.; Zimney, E. J.; Piner, R. D.; Dommett, G. H. B.; Evmenenko, G.; Nguyen, S. T.; Ruoff, R. S. Preparation and Characterization of Graphene Oxide Paper. *Nature* **2007**, *448*, 457–460.
30. Lee, D. H.; Kim, J. E.; Han, T. H.; Hwang, J. W.; Jeon, S.; Choi, S. Y.; Hong, S. H.; Lee, W. J.; Ruoff, R. S.; Kim, S. O. Versatile Carbon Hybrid Films Composed of Vertical Carbon Nanotubes Grown on Mechanically Compliant Graphene Films. *Adv. Mater.* **2010**, *22*, 1247–1252.